ELSEVIER

Biochimica et Biophysica Acta 1415 (1998) 174–180

BIOCHIMICA ET BIOPHYSICA ACTA

BBA

The lipid/protein interface as a target site for general anesthetics: a multiple-site kinetic analysis of synaptosomal Ca^{2+}-ATPase

Doris Pflugmacher, Heinrich Sandermann Jr. *

GSF-Forschungszentrum für Umwelt und Gesundheit GmbH, Institut für Biochemische Pflanzenpathologie, Ingolstädter Landstraße 1, D-85758 Oberschleißheim, Germany

Received 27 July 1998; received in revised form 28 September 1998; accepted 6 October 1998

Abstract

There is a long-standing controversy on whether membrane lipids or proteins are the target for general anesthetics. The plasma membrane-associated Ca^{2+}-ATPase of synaptosomes has recently been established as a model system for general anesthesia, the protein interior being the proposed target site (M.M. Lopez, D. Kosk-Kosicka, J. Biol. Chem. 270 (1995) 28239–28245). Multiple-site kinetics is now applied as a mechanistic tool to analyze inhibition by organic solvents and general anesthetics. A close fit to the experimental data points was achieved using the complex equations for a competitive displacement of lipid activators from multiple sites on the protein surface. Inhibitor dissociation constants were about 1.6×10^5-fold higher than the microscopic lipid dissociation binding constants that are derived here for the first time. Binding of lipid therefore is by −7.1 kcal/mole favored over that of the tested inhibitors. The latter are nevertheless effective because in the model used displacement of only few of the lipid solvation molecules cause complete inhibition. The lipid/protein interface rather than protein or lipid alone appeared to be the anesthetic target site.

Keywords: Lipid/protein interface; Anesthetic; Multiple-site; Kinetic analysis; Synaptosomal Ca^{2+}-ATPase; Ca^{2+}-ATPase

1. Introduction

There is a long-standing controversy on whether membrane lipids or proteins are the target for general anesthetics [1–3]. The displacement of solvation lipids by anesthetics has also been considered as a hypothetical mechanism [1,4]. The lipid/protein interface is a possible target site because many membrane enzymes [5,6] and gated channel proteins such as the nicotinic acetylcholine receptor [7,8] require lipids for activity. Electron spin resonance (ESR) spectroscopy with spin-labeled lipids appears to be the most appropriate method to directly examine displacement processes at the lipid/protein interface. However, such experiments have been stated to be technically very difficult [8] and have so far been both in favor of [9,10] and against [11,12] the lipid displacement mechanism. In view of the lack of adequate physical methods, multiple-site kinetics is employed here as a mechanistic tool. The present analysis is based on the kinetic formalism established previously for lipid-dependent enzymes [5,6] and for the inhibition of membrane enzymes by lipid displacement [13,14]. A re-

Abbreviations: I_{10}, I_{50}, I_{90}, inhibitor concentrations leading to 10%, 50%, and 90%, respectively, reduction of enzyme velocity; L_{10}, L_{50}, L_{90}, lipid concentrations to reach 10%, 50%, and 90%, respectively, of maximal lipid activation

* Corresponding author. Fax: +49 (89) 31873383; E-mail: sandermann@gsf.de

0005-2736/98/$ – see front matter
PII: S0005-2736(98)00187-4

cent stopped-flow kinetic study of the nicotinic acetylcholine receptor has shown that the cholesterol activation site is within, or very close to, the lipid/protein interface [15].

The elementary binding processes at the protein surface and the basic definitions of the microscopic lipid activator binding dissociation constant, K_l, and the microscopic inhibitor binding dissociation constant, K_i, are shown in Fig. 1. Probability factors have to be introduced when multiple binding sites are considered [5]. Theoretical modeling [13] and the analysis of the inhibition of $(Na^+ + K^+)$-ATPase and lactose permease by alcohols [14] have defined values of kinetic cooperativity that are diagnostic for the lipid displacement mechanism. The cooperativity index, $I_{90}/I_{10,}$ should be in the range between 2 and 30, a value of $I_{90}/I_{10} = 81$ representing hyperbolic kinetics. I_{90}/I_{10} is the ratio of inhibitor concentrations leading to 90% and 10% inhibition, respectively. The present kinetic analysis is based on the idea that catalytic membrane proteins require a defined number n of solvation lipid molecules for activity, although a number a of non-occupied lipid solvation sites may be tolerated [5].

Inhibition experiments and kinetic modeling are presented here for the synaptosomal Ca^{2+}-ATPase. Recent publications have established this enzyme as a model system for general anesthesia [16–18]. The enzyme is not of direct pharmacological relevance since the anesthetics were employed an order of magnitude above concentrations used in clinical practice

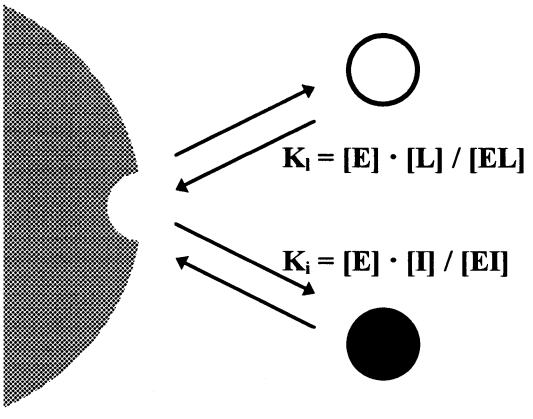

Fig. 1. Schematic view of the binding equilibria of lipid activator (○) and inhibitor (●) and definition of the elementary binding dissociation constants.

[19,20]. It was postulated that the hydrophobic protein interior acts as the anesthetic binding site, in analogy to the binding of anesthetics to the lipid-free proteins, myoglobin, hemoglobin and adenylate kinase [17]. The lipid displacement mechanism was not considered, but is now examined for organic solvents as well as general anesthetics. For this purpose, the published assay conditions [16–18] were adopted for the following strategy of kinetic analysis. (1) Activation kinetics: determine K_l for lipid activation of Ca^{2+}-ATPase, using a fixed value of n and a fitted value of a. (2) Inhibition kinetics: employ the values of K_l and a to derive K_i values for anesthetics and organic solvents. (3) Anesthetic efficiency: derive free energy differences of the binding of lipid activators versus anesthetic inhibitors from the numerical values of K_l and K_i by a standard thermodynamic treatment. Such free energy values are up to now not available in the literature.

2. Materials and methods

2.1. Synaptosomal plasma membranes

Cortical tissue of fresh pig brain from a Munich slaughterhouse was homogenized and synaptosomal plasma membranes were prepared by Ficoll gradient centrifugation, using published procedures [21]. The preparation was stored at −80°C. The lipid to protein ratio of synaptosomal plasma membranes is about 1:1 [22]. A uniform lipid molecular mass value of 800 Da was used for stoichiometric calculations. Protein was determined by the procedure of Bradford [23].

2.2. Enzyme assays

All assays were carried out in a final volume of 330 μl with use of 5 μg total plasma membrane protein. Ca^{2+}-ATPase activity was determined as described [18] without addition of calmodulin. Typical values of specific activity were 5–7 nkat/mg protein regardless of whether calmodulin (Sigma Cat. No. P1915) was added or not. Control values (subtracted) were determined in the presence of 1 mM EGTA. Liberated free phosphate was measured colorimetrically [24]. $(Na^+ + K^+)$-ATPase activity was determined as

described [18] using 72 mM histidine, 1.4 mM EGTA, pH 7.4, as test buffer. Control values (subtracted) were determined in the presence of 1 mM ouabain. Typical values of specific activity were 20–30 nkat/mg protein. Mg^{2+}-ATPase was determined as described [18] using 69 mM Tris-maleate, 1.4 mM EGTA, pH 7.4, as test buffer. Control values (subtracted) were determined without addition of Mg^{2+}. Typical values of specific activity were between 13 and 16 nkat/mg protein.

Ca^{2+}-ATPase activity was reduced by 45% upon inclusion of 1 mM vanadate. About 50% vanadate inhibition has previously been reported for rat cerebrum synaptosomal Ca^{2+}-ATPase [25]. Highly purified plasma membrane Ca^{2+}-ATPase is known to show maximally 80% inhibition by vanadate [26]. As in the previous studies [16–18,21] addition of vanadate was not made in the inhibition experiments to be described. The present Ca^{2+}-ATPase activity appears to differ from synaptosomal ecto-ATPases that are equally well activated by Ca^{2+} and Mg^{2+} and that are insensitive to vanadate [25,27]. The pig synaptosomal vesicles used here are known to contain plasma membrane Ca^{2+}- and Mg^{2+}-ATPases [21].

2.3. Inhibition experiments

The inhibitors were added to the assay mixtures (minus ATP) by means of Hamilton syringes. Enzyme assays were carried out in gas-tight HPLC vials carrying a septum. Alcohol concentrations were calculated from the added amounts. The other inhibitors were added in buffer that had been equilibrated with excess inhibitor. The following literature values [28] for aqueous saturation concentrations were used: chloroform, 66.6 mM; halothane: 17 mM; isoflurane: 15 mM; enflurane: 15 mM. Corrections of approx. 10% were made for losses into the vial head space. Justification for the procedures used here comes from the agreement of the present inhibition results with the previously reported data [16–20] where aqueous anesthetic concentrations had been calibrated by gas chromatography. After preincubating the present inhibitor-containing assay mixtures for 15 min at 37°C, the enzyme reactions were in all cases started by addition of ATP (dissolved in assay buffer) to a final concentration of 3 mM.

2.4. Data treatment

Three to nine replicates of all experiments were performed and mean values ± S.D. determined. All calculations, including non-linear regression were carried out using Sigma Plot software.

3. Results

3.1. Kinetics of lipid activation

No precise lipid activation data are available for the synaptosomal Ca^{2+}-ATPase, but this is the case for the structurally related plasma membrane-associated Ca^{2+}-ATPase from erythrocytes [29]. An initial kinetic analysis of these activation data had shown that the cooperativity index, L_{90}/L_{10}, was around 10 [6], and therefore within the range of L_{90}/L_{10} between 2 and 30 that is typical for activation by lipid solvation [5,6]. L_{90}/L_{10} is the ratio of lipid concentrations required to reach 90% and 10%, respectively, of maximum activation. The deduction of K_l values (see Fig. 1 for definition) requires knowledge of the total number n of lipid molecules solvating the enzyme molecule [30]. This value is not known for plasma membrane-associated Ca^{2+}-ATPases, but the modeling of lipid-dependent enzymes generally is not very sensitive to the exact value of n [30]. Therefore, the value of $n = 60$ that has been determined for $(Na^+ + K^+)$-ATPases by ESR spectroscopy [31] is adopted here in view of protein chemical similarities between plasma membrane Ca^{2+}- and $(Na^+ + K^+)$-ATPases [32]. The full rate equation of [5] was used. The non-linear regression analysis of activation by phosphatidylserine (Fig. 2A) led to an optimal value of 1 for the maximum number (a) of vacant lipid solvation sites that are tolerated by the enzyme. Values between 1 and 5 have previously been obtained for dogfish $(Na^+ + K^+)$-ATPase [30]. A satisfactory fit was reached with a lipid binding dissociation constant of $K_l = 0.16$ nmoles lipid per μg purified protein. With a molecular mass value of 280 kDa for the active Ca^{2+}-ATPase dimer [21,32], this corresponds to $K_l = 45$ lipid molecules per enzyme molecule (the dimension used previously [13]). Similar K_l values were obtained for the other lipid activators tested with erythrocyte Ca^{2+}-ATPase (phosphatidic

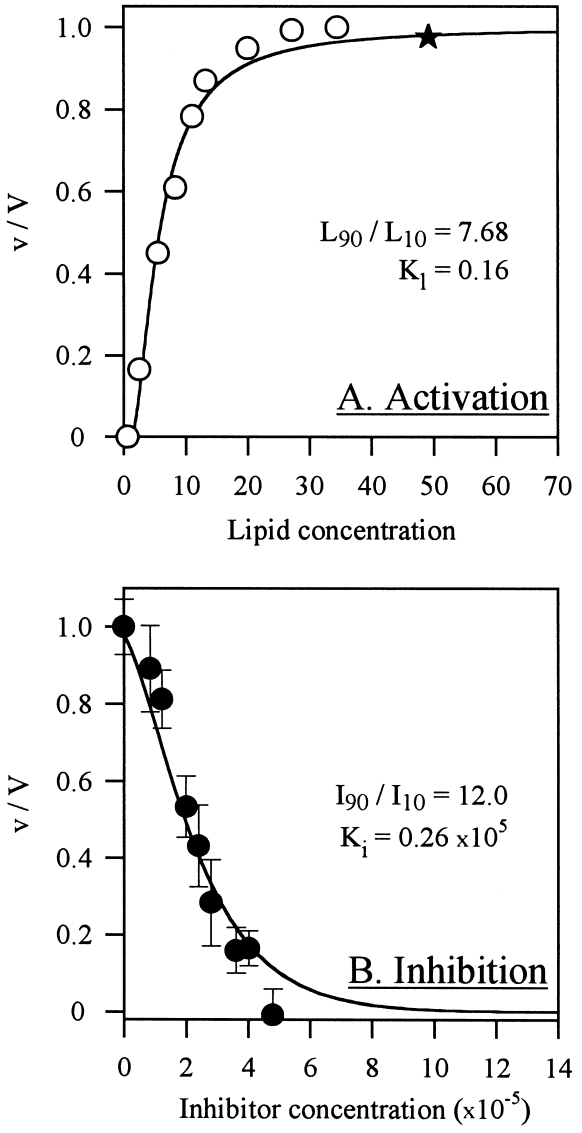

Fig. 2. Kinetic modeling of plasma membrane Ca^{2+}-ATPases. (A) Activation of the erythrocyte enzyme by phosphatidylserine. (B) Inhibition of the pig synaptosomal enzyme by chloroform. In order to be consistent with the published activation data [29], kinetic constants are given in units of nmol lipid or inhibitor per μg purified protein. Relative velocity is plotted as the ratio of actual over maximal velocity, v/V. Lipid activation was calculated using the full rate equation of [5] with values of $n=60$ and $a=1$, and using the published experimental data points (○) stimulation by phosphatidylserine [29]. A relative velocity of 0.98 (★) provided the starting point to calculate the inhibition curve in panel B. The values of n, a, and K_l from the activation curve were used to fit the experimental data points (●) for inhibition by chloroform. For the comparison with panel A, the millimolar inhibitor concentration unit of Table 1 was converted to the dimension of nmoles inhibitor/μg purified protein as follows. The amount of membrane protein used (5 μg) was divided by 300 in order to obtain the equivalent amount of purified Ca^{2+}-ATPase protein. Purification factors of about 300 have been reported for both the erythrocyte [29] and the synaptosomal [21] plasma membrane Ca^{2+}-ATPase. Next, the nmoles solvent or anesthetic were calculated from molarity in the test volume of 330 μl. One millimolar concentration unit corresponded to 2.1×10^4 nmoles inhibitor/μg purified protein. The inhibition curve and the derived K_i value are shown for the higher K_l value. The same ratio of K_i/K_l was obtained for both K_l values. The full rate equation of [5] was used, replacing K_l by $K_l' = K_l\times(1+[I]/K_i)$ (cf. [13]).
←

acid, phosphatidylinositol, cardiolipin [29]). These values appeared to be too high when compared to the common value of $K_l = 3.8\pm1.4$ lipid molecules per enzyme molecule that has been derived from lipid activation curves of dogfish $(Na^+{+}K^+)$-ATPase, sarcoplasmic reticulum Ca^{2+}-ATPase and yeast and bovine mitochondrial cytochrome oxidases (unpublished results). The latter value corresponds to $K_l = 0.014$ nmoles lipid per μg purified protein. The reason for the elevated K_l value of Fig. 2A is not clear. Lipid concentrations of up to 60 nmoles per μg purified protein were employed [29], but only about 1–1.3 nmoles lipid per μg protein are present

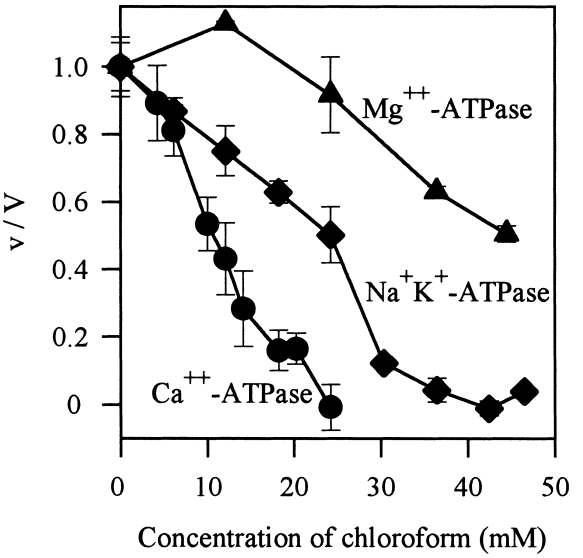

Fig. 3. Inhibition of the Mg^{2+}-, $(Na^+{+}K^+)$- and Ca^{2+}-ATPase activities of a pig synaptosomal plasma membrane preparation by chloroform. Relative velocity (v/V) is plotted versus concentration of chloroform (mM).

Table 1
Kinetic constants for the inhibition of the synaptosomal plasma membrane-associated Ca^{2+}-ATPase activity by organic solvents and general anesthetics

Inhibitor	I_{50} (mM)	I_{90}/I_{10}
Ethanol	360	6.2
Butanol-1	120	4.1
Hexanol-1	7.0	4.4
Chloroform	10.0	4.8
Enflurane	2.8	10.3
Isoflurane	1.9	n.d.
Halothane	2.1	4.4

All values were obtained by graphical analysis of inhibition curves of the type depicted in Fig. 3. n.d., not determined.

in plasma membranes from erythrocytes [33] and synaptosomes [22].

3.2. Kinetics of inhibition

When the three basic ATPase activities of synaptosomal membranes were tested in the presence of organic solvents, Ca^{2+}-ATPase activity was inhibited much more than the $(Na^+ + K^+)$-ATPase or Mg^{2+}-ATPase activities. This result is shown for chloroform in Fig. 3. The same result was obtained for hexanol-1, ethanol and butanol-1 (not shown), and has been reported before for halothane and isoflurane [18].

The half-maximal inhibitor concentration, I_{50}, and the cooperativity index, I_{90}/I_{10} were determined from the inhibition curves determined for Ca^{2+}-ATPase with a number of solvents and general anesthetics. These values are summarized in Table 1, and were in the cases of halothane, isoflurane and enflurane consistent with previously published inhibition curves [16–19]. There was a rough correlation between anesthetic potency and I_{50}. All values of I_{90}/I_{10} were within the range of 2–30 that is characteristic for the lipid displacement mechanism [14]. For a quantitative comparison with the lipid activation data, the millimolar concentration values of Table 1 had to be converted to the dimension of nmoles inhibitor/μg purified protein (Fig. 2B). Curve fitting with the values of $n=60$, $a=1$ led to K_i values of $0.22 \cdot 10^4$ and 0.6×10^5 nmoles inhibitor per μg purified protein for the low K_l and the high K_l value, respectively. The theoretical inhibition curve obtained for chloroform is shown in Fig. 2B. The ratio K_i/K_l amounted to 1.6×10^5 for both K_l values. The general relationship $\Delta G = -RT \times \ln(K_i/K_l)$ led to a free energy value of about −7.1 kcal/mole, so that the binding of chloroform (as well as of the inhibitors tested) is much less favorable than that of the lipid activators.

4. Discussion

By first analyzing published lipid activation data [29], a numerical framework was generated to also quantitatively analyze the experimental inhibition data. It has initially been reported that the inhibition of the Ca^{2+}-ATPase occurs in a range that is relevant for clinical anesthesia [16–19]. However, this conclusion has subsequently been ascribed to a calculation error by a factor of 10 [19,20]. The synaptosomal Ca^{2+}-ATPase should therefore be considered as a model system rather than a physiological target of general anesthesia.

The Ca^{2+}-ATPase had a much higher inhibitor sensitivity than the $(Na^+ + K^+)$- and Mg^{2+}-ATPases of the same synaptosomal membrane preparation (Fig. 3). A number of processes may be responsible, one factor being structural differences between the lipid/protein interfaces of the three tested ATPases. There may be especially sensitive interfacial sites, and the assumed identity of all sites [5,6,13,14] is certainly oversimplified. Furthermore, the assay conditions chosen are known to strongly influence anesthetic sensitivity. For example, $(Na^+ + K^+)$-ATPase activity measured as ouabain-sensitive influx of $^{86}Rb^+$ was highly sensitive to halothane, while standard $(Na^+ + K^+)$-ATPase enzyme assays were largely insensitive [34]. Ca^{2+}-ATPase pumping assays are also known to be sensitive to clinical concentrations of inhalational anesthetics [25]. Still, the reason for the high apparent anesthetic sensitivity of flux assays was not clarified. No attempt was made here to modify the less anesthetic-sensitive assay conditions of Kosk-Kosicka et al. [16–20], because the present results were to be compared to the previous data [16–18]. For the same reason, another possible improvement was not attempted, namely to work with defined isoenzyme forms of plasma membrane Ca^{2+}-ATPase [32,35]. Ca^{2+}-ATPase isoenzymes may conceivably differ in anesthetic sensitivity, as already

demonstrated for Ca^{2+} and calmodulin dependencies [35].

A number of $n = 60$ lipid solvation molecules per Ca^{2+}-ATPase dimer of 280 kDa was assumed here on the basis of protein chemical similarities between plasma membrane Ca^{2+}-ATPase and $(Na^{+}+K^{+})$-ATPase [32] and of ESR spectroscopic data for the latter enzyme [31]. The lipid displacement mechanism was supported by the finding that the cooperativity index, I_{90}/I_{10}, was in all cases within the characteristic range of 2–30 [14]. The differences between the values of L_{90}/L_{10} of 7.68 (Fig. 2A) and the various I_{90}/I_{10} values do not appear to be reliable. The analysis led to a marked energetic difference between the binding of lipid and of the tested anesthetics, the binding of lipid being favored by about −7.1 kcal/mole. This value may be compared to the much smaller value (−1.0 kcal/mole) for another, more subtle hydrophobic exchange reaction, namely the transfer of cholesterol from an isotropic lipid phase into an anisotropic phospholipid bilayer [36]. At first sight, the much less favorable binding of anesthetics suggests that anesthetic/protein interactions are too weak to be relevant. On the other hand, functional membrane proteins in the model used are extremely vulnerable to lipophilic inhibitors because only a small number of lipid molecules needs to be displaced for complete inactivation. More precisely, the threshold number for complete inhibition is $(a+1)$. The fit of the modeled inhibition curve of Fig. 2B documents that the model used is realistic.

The Ca^{2+}-induced enhancement of tryptophan fluorescence of the synoptosomal Ca^{2+}-ATPase has been found to be quenched by general anesthetics [17]. Our analysis of the published quenching curves led to I_{50} and I_{90}/I_{10} values close to those given for enzyme inhibition in Table 1. The similarity of the enzyme inhibition and fluorescence quenching curves for volatile anesthetics has previously been noted and interpreted in terms of the hydrophobic protein interior serving as the anesthetic binding site [17]. This hypothesis was based on an apparent analogy to the binding of anesthetics to the lipid-free proteins, myoglobin, hemoglobin and adenylate kinase. On the other hand, the interaction of these anesthetics with the synaptosomal Ca^{2+}-ATPase is driven by entropy, whereas the interaction of lipophilic compounds with myoglobin and adenylate kinase is known to be driven by enthalpy [37]. Lipid-free proteins may therefore not be good model systems for general anesthesia, as previously also concluded for luciferase on the basis of insufficient kinetic cooperativity [14].

Interactions at the lipid/protein interface have a large effect on protein conformation, as shown by the phenomenon of lipid activation [5–8]. A single amino acid residue deletion altered the lipid binding of a K^{+}-channel-associated peptide, as indicated by recent ESR spectroscopic experiments [38]. Similarly, site-directed mutagenesis or subunit exchange in gated ion channel proteins indicates that general anesthesia depends on specific amino acid residues that reside mostly in transmembrane helices [3,39–41]. Most authors are careful to note that it is still unknown whether such critical amino acids are part of the anesthetic binding site or of the transducing mechanism and to what degree the amino acid side-chains are in contact with lipids [39–41]. Some 30 published dose-response curves for the effects of general anesthetics on tadpoles, on desensitization of the nicotinic acetylcholine receptor and on various ion channels have been analyzed for kinetic cooperativity and found to be in all cases in the range of I_{90}/I_{10}, 2–15 (unpublished data). With multiple-site kinetics as a tool, the lipid displacement mechanism therefore appears to have general relevance. The cholesterol activator site of the nicotinic acetylcholine receptor also was within or very close to the lipid/protein interface [15]. However, direct physical methods suitable for a distinction between the lipid/protein interface and pure lipid or protein phases as target sites for general anesthetics need to be developed. ESR spectroscopy still presents great technical problems [8]. In summary, the results presented here provide good, albeit indirect, evidence for the lipid/protein interface rather than protein or lipid alone as a target site for general anesthetics.

Acknowledgements

Fruitful discussions with Prof. Keith W. Miller and members in his laboratory at the Massachusetts General Hospital (Boston, MA, USA) are gratefully acknowledged. This study has been supported in part by EUROSILVA and by the Fonds der Chemischen Industrie.

References

[1] K.W. Miller, Int. Rev. Neurobiol. 27 (1985) 1–61.
[2] N.P. Franks, W.R. Lieb, Nature 367 (1994) 607–614.
[3] R.W. Peoples, C. Li, F.F. Weight, Annu. Rev. Pharmacol. Toxicol. 36 (1996) 185–201.
[4] P. Seeman, Pharmacol. Rev. 24 (1972) 583–655.
[5] H. Sandermann, Eur. J. Biochem. 127 (1982) 123–128.
[6] H. Sandermann, in: A. Watts, J.J.H.H.M. De Pont (Eds.), Progress in Protein-Lipid Interactions, vol. 2, Elsevier, Amsterdam, 1986, pp. 197–220.
[7] L. Pradier, M.G. McNamee, in: P. Yeagle (Ed.), The Structure of Biological Membranes, CRC Press, Boca Raton, FL, 1992, pp. 1047–1106.
[8] K.W. Miller, in: S.A. Feldman, D. Paton, C. Scurr (Eds.), Mechanism of Drugs in Anesthesia, E. Arnold, London, 1995, pp. 181–200.
[9] D.M. Fraser, S.R.W. Louro, L.I. Horváth, K.W. Miller, A. Watts, Biochemistry 29 (1990) 2664–2669.
[10] C.M.B. Lopes, S.R.W. Louro, Biochim. Biophys. Acta 1070 (1991) 467–473.
[11] V.C. Abadji, D.E. Raines, A. Watt, K.W. Miller, Biochim. Biophys. Acta 1147 (1993) 143–153.
[12] V.C. Abadji, D.E. Raines, L.A. Dalton, K.W. Miller, Biochim. Biophys. Acta 1194 (1994) 25–34.
[13] H. Sandermann, Biochim. Biophys. Acta 1150 (1993) 130–133.
[14] H. Sandermann, D. Pflugmacher, Biochim. Biophys. Acta 1300 (1996) 219–225.
[15] G.H. Adonna, H. Sandermann, M.A. Kloczewiak, S.S. Husain, K.W. Miller, Biochim. Biophys. Acta 1370 (1998) 299–309.
[16] D. Kosk-Kosicka, G. Roszczynska G, Anesthesiology 79 (1993) 774–780.
[17] M.M. Lopez, D. Kosk-Kosicka, J. Biol. Chem. 270 (1995) 28239–28245.
[18] I. Fomitcheva, D. Kosk-Kosicka D, Anesthesiology 84 (1996) 1189–1195.
[19] M.M. Lopez, D. Kosk-Kosicka, J. Biol. Chem. 271 (1996) 26444.
[20] D. Kosk-Kosicka, Anesthesiology 85 (1996) 1211.
[21] J.M. Salvador, A.M. Mata, Biochem. J. 315 (1996) 183–187.
[22] G.B. Ansell, in: G.B. Ansell, R.M.C. Dawson, J.N. Hawthorne (Eds.), Form and Function of Phospholipids, Elsevier, Amsterdam, 1973, pp. 377–422.
[23] M. Bradford, Anal. Biochem. 72 (1976) 248–254.
[24] E.S. Baginsy, P.P. Foa, B. Zak, Clin. Chim. Acta 15 (1967) 155–158.
[25] J.J. Franks, J.-L. Horn, P.K. Janicki, G. Singh, Anesthesiology 82 (1995) 108–117.
[26] E. Carafoli, M. Zurini, Biochim. Biophys. Acta 683 (1982) 279–301.
[27] A.K. Nagy, T.A. Shuster, A.V. Delgado-Escueta, J. Neurochem. 47 (1986) 976–986.
[28] L.L. Firestone, J.C. Miller, K.W. Miller, in: S.H. Roth, K.W. Miller (Eds.), Molecular and Cellular Mechanisms of Anesthetics, Plenum, New York, 1986, pp. 455–470.
[29] V. Niggli, E.S. Adunyah, E. Carafoli, J. Biol. Chem. 256 (1981) 8588–8592.
[30] H. Sandermann, B.A. Gottwald, Biochim. Biophys. Acta 732 (1983) 332–335.
[31] D. Marsh, in: A. Watts (Ed.), Protein-Lipid Interactions. New Comprehensive Biochemistry, vol. 25, Elsevier, Amsterdam, 1993, pp. 41–66.
[32] E. Carafoli, FASEB J. 8 (1994) 993–1002.
[33] P.F. Devaux, M. Seigneuret, Biochim. Biophys. Acta 822 (1985) 63–125.
[34] S. Molliex, B. Dureuil, M. Aubier, G. Friedlander, J.-M. Desmonts, C. Clerici, Anesthesiology 88 (1998) 1606–1613.
[35] N.L. Elwess, A.G. Filoteo, A. Enyedi, J.T. Penniston, J. Biol. Chem. 272 (1997) 17981–17986.
[36] H. Sandermann, G.H. Addona, K.W. Miller, Biochim. Biophys. Acta 1346 (1997) 158–162.
[37] M.M. Lopez, D. Kosk-Kosicka, Biochemistry 36 (1997) 8864–8872.
[38] L.I. Horváth, P.F. Knowles, P. Kovachev, J.B.C. Findlay, D. Marsh, Biophys. J. 73 (1997) 2588–2594.
[39] P.A. Davies, M.C. Hanna, T.G. Hales, E.F. Kirkness, Nature 385 (1997) 820–823.
[40] S.J. Mihic, Q. Ye, M.J. Wick, V.V. Koltchine, M.D. Krasowski, S.E. Finn, M.P. Mascia, C.F. Valenzuela, K.K. Hanson, E.P. Greenblatt, R.A. Harris, N.L. Harrison, Nature 389 (1997) 385–389.
[41] D. Belelli, J.J. Lambert, J.A. Peters, K. Wafford, P.J. Whiting, Proc. Natl. Acad. Sci. USA 94 (1997) 11031–11036.